ISSN: 2588-4115; Infection Epidemiology and Microbiology. 2026;12(1):37-52 10.52547/iem.12.1.37

In-Silico Identification of Phytochemical Inhibitors of *Mycobacterium tuberculosis* Efflux Pumps: A Potential Strategy against Multidrug Resistance

ARTICLE INFO

Article Type
Original Article

Authors
Seyed Akbar Moosavi, *PhD*[1*]
Abdorrahim Absalan, *PhD*[1*]
Zahra Absalan, *PhD*[2]
Fereshteh Parto, *MSc*[1]

[1] Department of Medical Laboratory Sciences, School of Allied Medical Sciences, Iran University of Medical Sciences and Health Services, Tehran, Iran
[2] Department of Microbiology, Faculty of medicine, Ahvaz Jundishapur University of Medical Sciences, Ahvaz, Iran

** Correspondence*
Department of Medical Laboratory Sciences, School of Allied Medical Sciences, Iran University of Medical Sciences and Health Services, Tehran, Iran
E-mail: moosavi.a@iums.ac.ir
Department of Medical Laboratory Sciences, School of Allied Medical Sciences, Iran University of Medical Sciences and Health Services, Tehran, Iran
Email: absalan.a@iums.ac.ir

How to cite this article
Moosavi S.A., Absalan A., Absalan Z., Parto F. In-Silico Identification of Phytochemical Inhibitors of Mycobacterium tuberculosis Efflux Pumps: A Potential Strategy against Multidrug Resistance. Infection Epidemiology and Microbiology. 2026;12(1): 37-52.

Article History
Received: May 24, 2025
Accepted: January 27, 2026
Published: May 26, 2026

ABSTRACT

Background: Efflux pump-mediated antibiotic extrusion is a key mechanism of multidrug resistance in *Mycobacterium tuberculosis* (MTB). Inhibiting these pumps is a promising strategy for resensitizing resistant strains to conventional antibiotics.
Materials & Methods: An integrated *in silico* approach was employed to evaluate the interaction of drug-like ligands, primarily phytochemicals, with key MTB efflux pumps. Homology models of DrrA, DrrB, and DrrC proteins and the crystal structure of Rv1819c were used for molecular docking. Top-scoring ligands were subsequently analyzed for drug-likeness, toxicity profile, and binding stability via molecular dynamics (MD) simulations to identify the most promising efflux pump inhibitors (EPIs).
Findings: Molecular docking revealed high-affinity binding of several phytochemicals. The top-scoring ligands were curcumin, rosmarinic acid, and pracinostat for DrrA; curcumin, kanzonol C, and Skf-100330A for DrrB; and rosmarinic acid, curcumin, and kanzonol C for DrrC. For the Rv1819c protein, the top-scoring compounds were crocetin, curcumin, and kanzonol C, which were found to bind specifically to the ATP-interacting pocket. An integrated analysis of docking affinity, molecular dynamics stability, toxicity, and drug-likeness identified curcumin, kanzonol C, rosmarinic acid, and crocetin as the most promising candidate EPIs.
Conclusion: The present *in-silico* study identified curcumin, kanzonol C, rosmarinic acid, and crocetin as promising phytochemical inhibitors of key MTB efflux pumps. These compounds exhibited potential for synergistic activity with conventional anti-tuberculosis drugs. Therefore, preclinical and experimental validation is warranted to confirm their efficacy as efflux pump inhibitors.

Keywords: ATP-binding cassette transporters, Tuberculosis, Multidrug resistance, Molecular docking simulations, Phytochemicals

CITATION LINKS

[1] Remm S, Earp JC, Dick T, Dartois V, Seeger MA. Critical discussion on drug efflux in... [2] World Health Organization. Global tuberculosis report 2024... [3] Laborda P, et al. Role of bacterial ... [4] Duda-Madej A, et al. The impact of plant-derived... [5] Sowajassatakul A, et al. Overexpression of eis... [6] Choudhuri BS, et al. Overexpression and functional... [7] Khosravi AD, et al. Comparison of drrA and... [8] Zheng M, Lupoli T. Counteracting antibiotic resistance... [9] Compagne N, da Cruz AV, Müller R, Hartkoorn RC, Flipo M, Pos KM. Update on the... [10] Schwede T, Kopp J, Guex N, Peitsch MC. SWISS-MODEL: An automated protein... [11] Grimsey EM, Piddock LJ. Do phenothiazines possess antimicrobial and... [12] Rempel S, Gati C, Nijland M, Thangaratnarajah C, Karyolaimos A, de Gier JW, et al. A mycobacterial... [13] Arnittali M, Rissanou AN, Harmandaris V. Structure of biomolecules... [14] Devita N. World TB Day 2025: Advancing the... [15] Barua N, Buragohain AK. Therapeutic potential of... [16] Lara-Espinosa JV, et al. Effect of... [17] Wang D, Liang J, Zhang J, Wang Y, Chai X. Natural chalcones in... [18] Sarkar N, Khanal P, Rawat R, Dey YN, Roy KK. Rosmarinic acid and... [19] Venugopal A, Bryk R, Shi S, Rhee K, Rath P, Schnappinger D, et al. Virulence of... [20] Drumm JE, Mi K, Bilder P, Sun M, Lim J, Bielefeldt-Ohmann H, et al. Mycobacterium tuberculosis... [21] Glass LN, Swapna G, Chavadi SS, Tufariello JM, Mi K, Drumm JE, et al. Mycobacterium... [22] Pradhan S, Nautiyal V, Dubey R. Molecular docking of some... [23] Hussain S, Haq A, Nisar M, Ahmad T, Bhardwaj P. Evaluation of... [24] Negi N, Prakash P, Gupta ML, Mohapatra TM. Possible role of... [25] Ekambaram SP, Paramasivam S, Perumal SS, Dhakshinamurthy SS. Rosmarinus officinalis L.: A source of...

Introduction

Tuberculosis (TB), caused by the intracellular pathogen *Mycobacterium tuberculosis* (MTB), remains a leading cause of mortality among the top ten causes of death worldwide [1]. In 2021 alone, an estimated 10.6 million new cases and 1.6 million deaths were reported [2]. According to the World Health Organization (WHO) Global Tuberculosis Report 2024, the initial targets of a 50% reduction in TB incidence and a 75% reduction in mortality by 2025 (relative to 2015 levels) are unlikely to be achieved. Recent epidemiological trends indicate a concerning rise in TB cases, with 10.8 million people worldwide infected in 2023, compared to 10.7 million in 2022, 10.4 million in 2021, and 10.1 million in 2020. Achieving universal access to TB prevention, diagnosis, treatment, and care is projected to require US$22 billion annually by 2027, with an additional US$5 billion per year needed to support TB research efforts [2].

A major challenge in TB control is multidrug-resistant TB (MDR-TB), characterized by resistance to at least isoniazid and rifampicin. MDR-TB poses a significant public health threat due to limited therapeutic options, prolonged treatment regimens, increased toxicity of second-line drugs, and suboptimal treatment outcomes. The emergence of resistance is further exacerbated by the pathogen's ability to develop novel antibiotic evasion strategies. Among these strategies, efflux pumps (EFPs) play a critical role by actively extruding antimicrobial agents, thereby reducing their effective intracellular concentrations [3]. Among the various efflux systems in MTB, the *drrA-drrB-drrC* operon and the Rv1819c protein are of particular interest. The *drrA* (Rv2936) and *drrB* (Rv2937) genes encode components of an ATP-binding-cassette (ABC) transport system, where DrrA functions as the nucleotide-binding domain, and DrrB constitutes part of the membrane-spanning domain. The associated *drrC* (Rv2938) gene encodes a regulatory component believed to enhance pump activity [1]. Additionally, Rv1819c facilitates the transport of diverse compounds, including antibiotics and metabolic intermediates [4]. These efflux systems have been directly linked to resistance against rifampicin, isoniazid, fluoroquinolones, aminoglycosides, and other second-line agents [5]. Approximately 2.5% of the MTB genome is dedicated to genes encoding ABC transporters, a major class of efflux pumps [6]. Notably, *drrA* and *drrB* are significantly overexpressed in MDR-TB, whereas their expression remains low in drug-sensitive clinical isolates [7].

In recent years, efflux pump inhibition (EPI) has emerged as a promising adjuvant strategy to combat drug-resistant pathogens. By blocking these pumps, intracellular antibiotic concentrations could be restored to bactericidal levels, effectively resensitizing bacteria to conventional antimicrobials. However, currently available synthetic EPIs (e.g., verapamil and reserpine) often exhibit off-target effects, toxicity, and poor specificity. In contrast, phytochemicals represent a structurally diverse and pharmacologically promising source of potential EPIs. Alkaloids, flavonoids, terpenoids, and polyphenols have demonstrated antimicrobial and resistance-modulating effects in various bacteria, including MTB [8, 9]. Many of these compounds also possess favorable safety profiles and broad pharmacological versatility. Nevertheless, the precise mechanisms by which phytochemicals interact with mycobacterial efflux systems remain poorly understood.

In silico drug discovery methods, notably molecular docking and dynamics simulations, enable efficient and high-throughput screening of potential inhibitors by predicting binding affinities and simulating biomo-

lecular interactions. Although both small molecules and peptides have been widely explored as efflux pump inhibitors (EPIs) in various studies [8], small molecules have been shown to be superior candidates due to their greater stability, enhanced cellular permeability, and simpler logistical handling compared to peptides, which are susceptible to enzymatic degradation. These computational approaches are invaluable preclinical tools that provide a cost-effective and rational framework to guide hypothesis-driven research, especially when experimental methods are impractical or prohibitively expensive.

Objectives: In the present study, an integrated computational approach was employed to evaluate the ability of selected phytochemicals to bind and inhibit four critical MTB EFPs: DrrA, DrrB, DrrC, and Rv1819c. The findings may provide a molecular basis for developing innovative combination therapies that synergize conventional anti-TB drugs with phytochemical adjuvants.

Materials and Methods

Overall strategy and workflow: To identify optimal inhibitors of MTB EFPs, the following integrated bioinformatics workflow was implemented:

1. Target selection and preparation: Key ABC efflux proteins were selected based on their established role in multidrug resistance and evidence from previous experimental studies. The tertiary structures of the selected target proteins were subsequently simulated using the SWISS-MODEL server.
2. Virtual screening: A library of phytochemicals was screened against the prepared target proteins via molecular docking using Molegro Virtual Docker to identify high-affinity small molecule binders.
3. Binding stability assessment: Top ligand-protein complexes selected based on the primary screening process underwent validation through complementary docking studies and molecular dynamics simulations conducted using myPrestoPortal to evaluate binding stability and interactions.
4. Toxicity, drug-likeness, and target profiling: The absorption, distribution, metabolism, excretion, and toxicity (ADMET) profiles of the lead candidates were predicted using T.E.S.T. and Toxtree software and the PubChem database. Their biological targets were also predicted using the SwissTargetPrediction server.
5. Candidate prioritization and data synthesis: A multi-parameter scoring system was applied to rank the compounds. The results were interpreted to propose the best-performing phytochemical candidates as inhibitors of MTB EFPs.

Selection of EFPs and tertiary structure modeling: The ABC transporter proteins DrrA and DrrB were selected as primary targets in this study based on their previously demonstrated critical role in anti-MTB drug efflux [7]. To identify additional relevant proteins, the STRING database (https://string-db.org/) was searched for functional partners. This analysis revealed DrrC as the most strongly-associated protein, exhibiting the highest co-expression rate with DrrA and DrrB in MTB H37Rv strain. Therefore, DrrC was included as a third target in subsequent *in silico* investigations.

The tertiary structures of the daunorubicin-transport ATP-binding proteins DrrA, DrrB, and DrrC in MTB were predicted using the SWISS-MODEL homology modeling server (https://swissmodel.expasy.org/). Validation of SwissModel homology models was performed based on the global model quality estimation (GMQE) score and the percentage of sequence identity (SID) with the template protein structures. A model was considered highly reliable when its GMQE score was > 0.7 or its sequence identity with the template was > 50% [10]. The resulting

structures were downloaded in PDB format for subsequent molecular docking studies.

Screening and selection of compounds: A ligand library consisting of 62 compounds was assembled for initial screening (please, see data availability). The library comprised 56 natural phytochemicals, five known synthetic EPIs, and pracinostat, a drug used for the treatment of leukemia. Initial virtual screening was performed against the modeled structure of the DrrA protein using Molegro Virtual Docker 6.0 (CLC bio).

Based on the resulting docking scores, 14 top-performing compounds were selected for further evaluation against the modeled DrrB and DrrC structures and a known MTB ABC transporter structure. The initial list of candidates included: 6-Dpg, chlorogenic acid, crocetin, curcumin, kanzonol B, kanzonol C, piperine, pracinostat, reserpine, rosmarinic acid, Skf-100330A, thioridazine, verapamil, and vulgaxanthin. From this list, verapamil (454.6 g/mol) and reserpine (608.7 g/mol) were excluded from further analysis as their molecular weights exceeded the 400 Da threshold imposed by myPrestoPortal software for molecular dynamics simulations. Thioridazine (370.6 g/mol) was selected as a representative synthetic control EPI for subsequent analyses based on its superior docking score and acceptable molecular weight [11].

Molecular docking with Rv1819c: To assess the binding potential of the selected compounds to a critical site within a known MTB efflux pump, a molecular docking study was performed against the Rv1819c ABC transporter. The high-resolution crystal structure of Rv1819c (PDB ID: 6TQE), determined by electron microscopy at a resolution of 4.30 Å and expressed in *Escherichia coli* [12], was retrieved from the Protein Data Bank . The docking screen included the following compounds: 6-Dpg, chlorogenic acid, crocetin, curcumin, kanzonol B, kanzonol C, piperine, pracinostat, rosmarinic acid, Skf-100330A, thioridazine, and vulgaxanthin. The highest binding affinities were observed for crocetin, curcumin, and kanzonol C. Notably, the most favorable docking scores were associated with the ATP-binding site located in the intracellular domain of the protein.

Molecular dynamics simulations: Based on the docking results**,** molecular dynamics (MD) simulations were conducted to evaluate the stability of the complexes formed between the top-scoring ligands (crocetin, curcumin, and kanzonol C) and each target protein (DrrA, DrrB, and DrrC). For comparative purposes, simulations were also performed for the control compound, thioridazine. All simulations were executed using myPrestoPortal version 1.1.88 (Japan Biological Informatics Consortium, JBIC), a graphical user interface (GUI) for the myPresto and GROMACS software suites. The system was first energy-minimized using the generalized born method for 5,000 steps. Production MD runs were then performed for 200 picoseconds with a loop limit of 100,000 steps. The trajectories were analyzed by monitoring changes in energy, temperature, and root-mean-square deviation (RMSD). Since the energy and temperature profiles remained stable across simulations, subsequent analyses focused primarily on RMSD to assess the stability of the ligand-protein complexes.

ADME, toxicity, and target prediction: The drug-likeness of the selected chemical compounds was evaluated according to Lipinski's rule of five (RO5). The physicochemical properties of each compound were retrieved from PubChem. Structure-activity relationships and toxicity profiles were predicted using Toxtree (estimation of toxic hazard - a decision tree approach, Version 3.1.0) and T.E.S.T. (Toxicity Estimation Software Tool, Version 5.1.2, U.S. Environmental Protection Agency). Potential biological targets were identified using the SuperPred server.

Development of a comparative decision score: To enable a comparative analysis of the compounds based on their drug-likeness and toxicity profiles, a multi-parameter scoring system was developed. A compound was considered more favorable if it exhibited the following characteristics: 1) improved drug-likeness: lower values for molecular weight, XLogP3, number of hydrogen bond donors and acceptors, number of rotatable bonds, total polar surface area (TPSA), and heavy atom count; 2) reduced toxicity: higher oral rat LD_{50}, higher bioconcentration factor, absence of developmental toxicity or mutagenicity, low toxicity class, high biodegradability, and metabolism by cytochrome P450; 3) favorable absorption: higher solubility at 25 °C; and 4) no structural alerts: no alerts for promiscuous protein binding, DNA binding, or carcinogenicity.

Given the challenge of visually interpreting complex, multi-parameter data, a qualitative three-color heat-map was generated in Microsoft Excel 2019 (conditional formatting → color scales) to provide an intuitive overview (green: optimal, pink: intermediate, and red: suboptimal). However, to address the need for a rigorous and objective metric that avoids visual subjectivity, this qualitative data was converted into a quantitative decision score using the following formula:

Decision Score = (Σ [pink cells + red cells] + targets count) - (Σ green cells)

In this formula, the target count represents the number of biological targets identified by the SuperPred server, integrating polypharmacology into the assessment. This scoring system was specifically designed to ensure that a lower numerical value unambiguously indicates a more promising candidate, thereby providing a single, objective benchmark for ranking all compounds.

Statistical analysis: Molecular docking scores (MolDock scores: DSC) of the 12 studied compounds were compared using one-way analysis of variance (ANOVA); a *p*-value < .05 was considered statistically significant. For conciseness, post-hoc comparisons of the scores of each compound against the control (thioridazine) were reported. For each compound, the minimum docking energy (the most negative value) represented

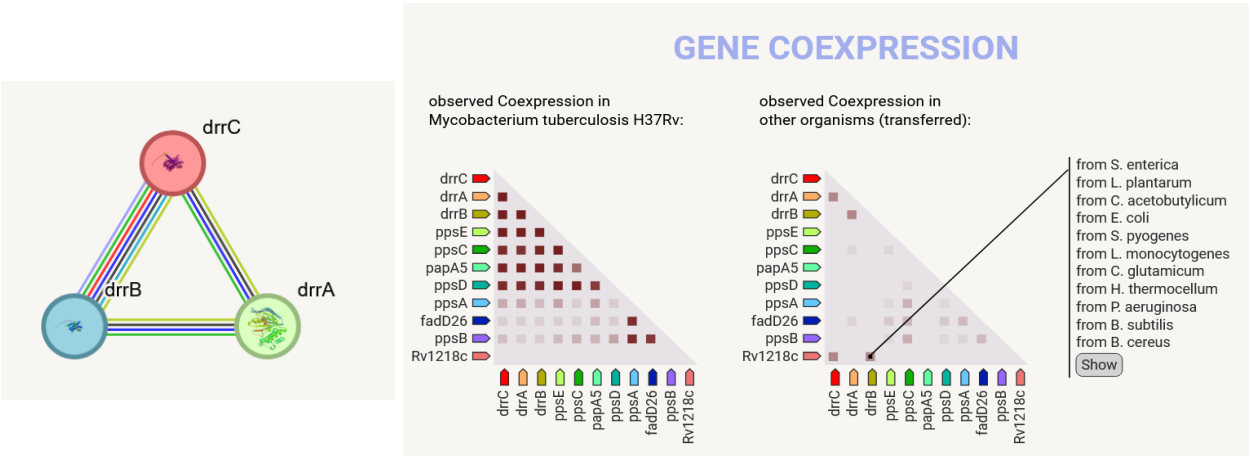

Figure 1) STRING-db analysis of EFP associations in MTB-H37Rv. The network illustrates the functional partners of DrrA and DrrB, identifying DrrC as the most closely associated protein with the highest co-expression score (left-hand graph and network). This strong co-expression pattern is not observed in other bacterial genera (right-hand graph), indicating its specificity to MTB. The lines connecting the nodes represent the evidence for each interaction, as defined by the STRING database: curated databases (pink), experimentally determined (green), predicted interactions (blue), gene neighborhood (red), gene fusions (purple), gene co-occurrence (orange), and text-mining (yellow). In the co-expression graph, the deep-brown color represents a higher confidence score.

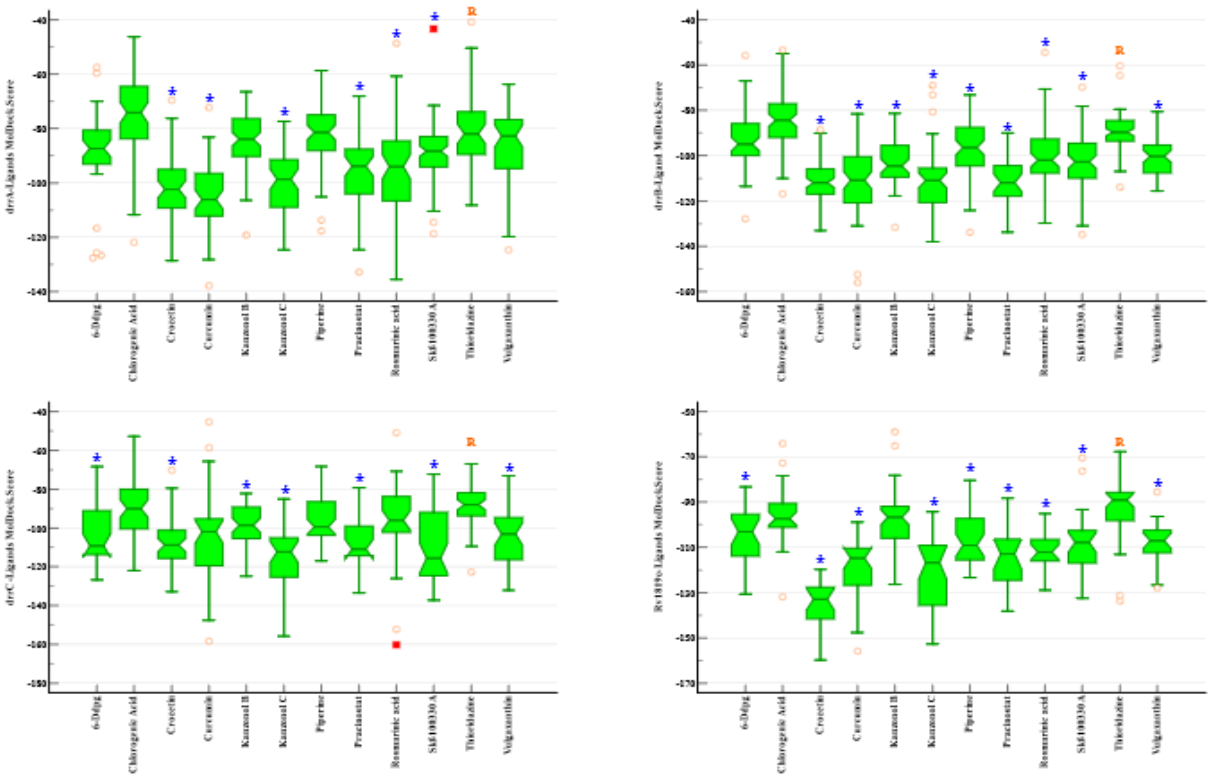

Figure 2) Comparative DSCs of the 12 evaluated compounds docked against the DrrA, DrrB, DrrC, and Rv1819c proteins. DSC for the reference ligand, thioridazine (a known efflux pump inhibitor), is marked by the red R word. Significant differences ($p < .05$, ANOVA) compared to thioridazine are indicated by a blue asterisk (*). The three top-scoring ligands for each target were curcumin, rosmarinic acid, and pracinostat for DrrA; curcumin, kanzonol C, and Skf-100330A for DrrB; rosmarinic acid, curcumin, and kanzonol C for DrrC; and andcrocetin, curcumin, and kanzonol C for Rv1819c.

Table 1) Molecular docking analysis of phytochemical and chemical agents with *Mycobacterium tuberculosis* proteins DrrA, DrrB, DrrC, and Rv1819c. This table presents the number of binding poses per agent, the optimal docking score, hydrogen bond interactions at the primary pose, and common binding site residues across all 12 agents.

Protein	Phyto/Chemical Agent	NO. of Poses	Best Docking Score	Hydrogen Bond	Common Residues
DrrA	Curcumin	49	-137.87	Gln 158, Arg 82, and Ser 56	Gln 158, Arg 82, and Ile 84, Asp 150, Val 86, Trp 110, Val 157
	Rosmarinic acid	62	-135.53	Gln 158, 2Arg 82, Arg 81, Ile 84, and Trp 110	
	Pracinostat	54	-132.81	Ile 84, Pro 159, and 2Val 157	
	Crocetin	48	-128.64	2Gln 90	
	6-Dpg.	41	-127.69	Arg 82	
	Kanzonol C	55	-124.65	Ile 84, Arg 82, Gln 158	
	Vulgaxanthin	48	-124.63	Val 86, Asp 150, Cys 153, Val 157, Arg 82, Ile 84	
	Chlorogenic acid	62	-121.86	2Asp 150, 2Arg 82, Gln 158, 5Val 86, Trp 110	
	Kanzonol B	80	-119.15	Val 156, Val 157, Ile 84, Gly 154	
	Skf-100330A	83	-118.65	Val 86, Gly 88	
	Piperine	61	-117.72	No hydrogen bound	
	Thioridazine	47	-108.21	No hydrogen bound	

Protein	Phyto/Chemical Agent	NO. of Poses	Best Docking Score	Hydrogen Bond	Common Residues
DrrB	Curcumin	70	-156.04	3Asn 119, Arg 109	Ala 181, Arg 109, Arg 136, Arg 245, Asn 119, Ser 256
	Kanzonol C	53	-138.01	Ser 114, Thr 192, Arg 136	
	Skf-100330A	70	-134.76	Ala 181	
	Pracinostat	30	-133.78	Ala 181, Phe 185	
	Piperine	72	-133.77	No hydrogen bound	
	Crocetin	66	-133.07	Arg 109	
	Kanzonol B	53	-131.69	Thr 259. 2Gln 88, Gly 249, Arg 245, Ser 256	
	6-Dpg	55	-127.84	No hydrogen bound	
	Rosmarinic acid	64	-129.75	2Thr 51, 3Thr 52	
	Chlorogenic acid	70	-116.88	Ser 256, 2Tyr 89, Arg 245	
	Vulgaxanthin	51	-115.59	Met 125, Met 127, Phe 122, Pro 129, Leu 133, 3Arg 136, Asn 119	
	Thioridazine	77	-113.86	No hydrogen bound	
DrrC	Rosmarinic acid	34	-160.09	Gly 18, Arg 121, Pro 118, His 120, Gln 29, Ser 123, 2Gln 33, Leu 114, and Gly 124	Gly 18, Gly 124, Arg 121, Arg 104, Gln 33, Gln 29, Ser 123, Thr 47, Asp 101
	Curcumin	41	-158.44	Gly 124, Leu 16, Gly 18, Gln 33, Gln 29, Ser 123, and Arg 121	
	Kanzonol C	34	-155.75	Asp 101	
	Skf-100330A	44	-137.23	Gly 18, Pro 118, Gln 29	
	Pracinostat	23	-133.47	Arg 236, Thr 74, Ser 77	
	Crocetin	43	-132.82	No hydrogen bound	
	Vulgaxanthin	34	-132.09	Arg 104, Ile 46, Thr 47, 2Asp 101, Asp 44, Ala 131	
	6-Dpg	33	-126.73	Arg 104, Thr 47	
	Kanzonol B	50	-124.84	Thr 47, Phe 97, Asp 101	
	Thioridazine	50	-122.72	No hydrogen bound	
	Chlorogenic acid	50	-121.98	Asp 44, 2Thr 47, Trp 41, Leu 37, 2Asp 101, Val 98, Arg 128	
	Piperine	50	-116.96	Gln 29	
Rv1819c	Crocetin	21	-159.74	Gly 576, 2Arg 608, Thr 578	Arg 471, Arg 608, Gln 498, Gln 557, Gly 463, Gly 465, Gly 576, Gly 554, Lys 466, His 607, Ser 552, Ser 579, Thr 578, Thr 468, Thr 467, Val 605
	Curcumin	31	-155.85	3Arg 608, Gln 498, Lys 466, Thr 468	
	Kanzonol C	33	-152.68	Ser 552, Gly 554, Thr 467, Gln 498, Lys 466, His 607, and Val 605	
	Pracinostat	18	-138.16	2Ala 548, 2Arg 471, Lys 466, 2Thr 467	
	Thioridazine	39	-133.59	His 607	
	Skf-100330A	27	-132.44	Ser 579, Gln 557	
	Chlorogenic acid	32	-131.83	4Arg 608, 3Thr 578, 4Gly 576, Val 605, 4Ser 579, Gln 557, Pro 553	
	6-Dpg	26	-130.63	His 607, 2Thr 467	
	Rosmarinic acid	20	-128.89	3Arg 471, 2Thr 468, 2Gly 465, 2Gly 463, Lys 466, 2Glu 298	
	Vulgaxanthin	21	-127.79	Lys 466, Thr 467, Gly 463, Val 605, 2Gly 576, Thr 578, Gly 554, Ser 552, 3Gln 498	
	Kanzonol B	46	-126.32	Lys 466, Gly 465, 2His 607, Ser 462, Ser 552, Gly 554	
	Piperine	36	-123.34	Arg 608, Gly 554, Ser 552	

the most favorable binding conformation.

Findings

Efflux protein selection: Analysis of the STRING database to identify genes most closely associated with *drrA* and *drrB* revealed *drrC* as the top candidate in *M. tuberculosis* H37Rv strain, based primarily on its high co-expression level. This strong association appears to be specific to MTB, as supporting evidence in other organisms is limited (Figure 1).

Homology modeling: In this study, the optimal model for DrrA, generated using 16,325 templates (the top 50 were used), had a GMQE score of 0.89 and an SID of 85.20%. The DrrB model, generated using 183 templates (the top 50 were used), had a GMQE score of 0.81 and an SID of 71.73%. For DrrC, the model generated using 173 templates (the top 50 were used) yielded a GMQE score of 0.9 and an SID of 78.99%. Details of homology modeling are available as noted in data availability section.

Molecular docking results: The comparative docking results of all 12 compounds against the four target proteins (DrrA, DrrB, DrrC, and Rv1819c) are summarized in Figure 2. Detailed data, including the number of binding poses per compound, optimal docking score, hydrogen bond interactions in the top-ranked pose, and common binding site residues across all agents, are provided in Table 1.

The binding interactions of the top three ligands and the control agent (thioridazine) are shown in Figures 3A, 3B, and 3C. These figures depict the structures of the modeled proteins, their binding sites, and their key interacting amino acid residues.

For the Rv1819c protein (PDB: 6TQE), the top-performing ligands primarily interacted within a region identified as the ATP-binding site. Figure 4A shows a representative docking pose at this site, and the detailed

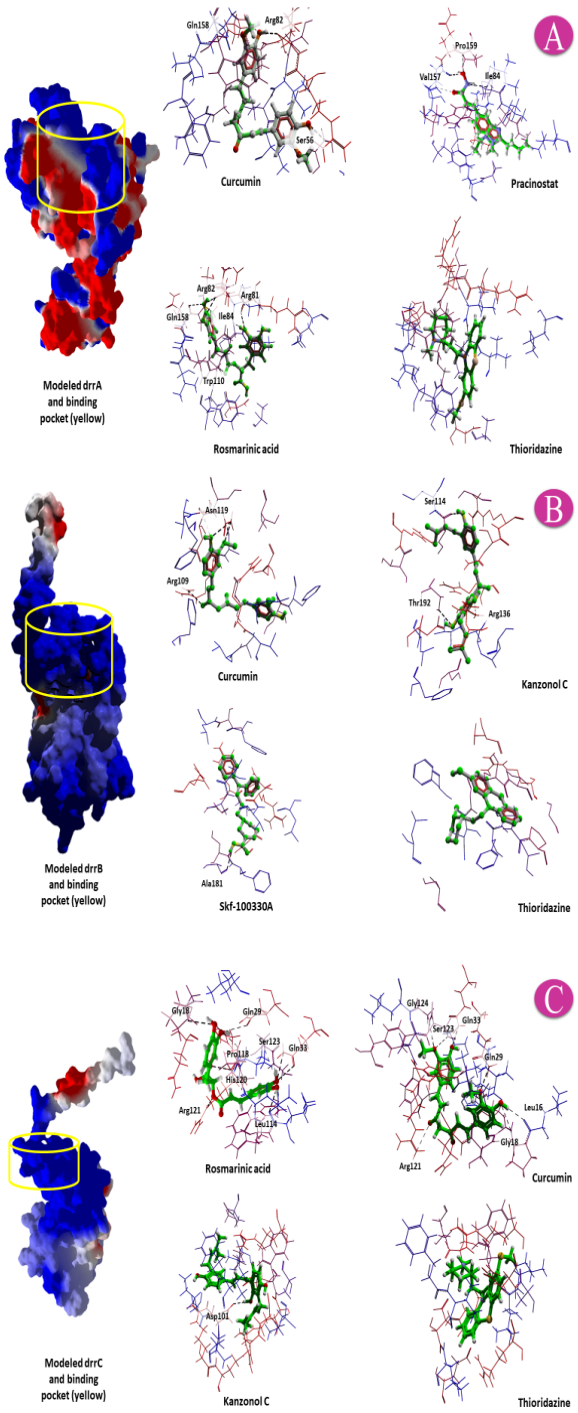

Figure 3) Molecular docking poses and interactions of top-scoring ligands with modeled Drr proteins. The binding pocket of each protein is outlined in yellow. Hydrogen bonds are depicted as black dashed lines, with thicker lines indicating stronger interactions. The top three compounds and the control (thioridazine) are shown for (A) DrrA, (B) DrrB, and (C) DrrC. Thioridazine formed no hydrogen bonds with any of the Drr proteins. The minimum DSC for the top ligands is provided for each protein (see Findings section).

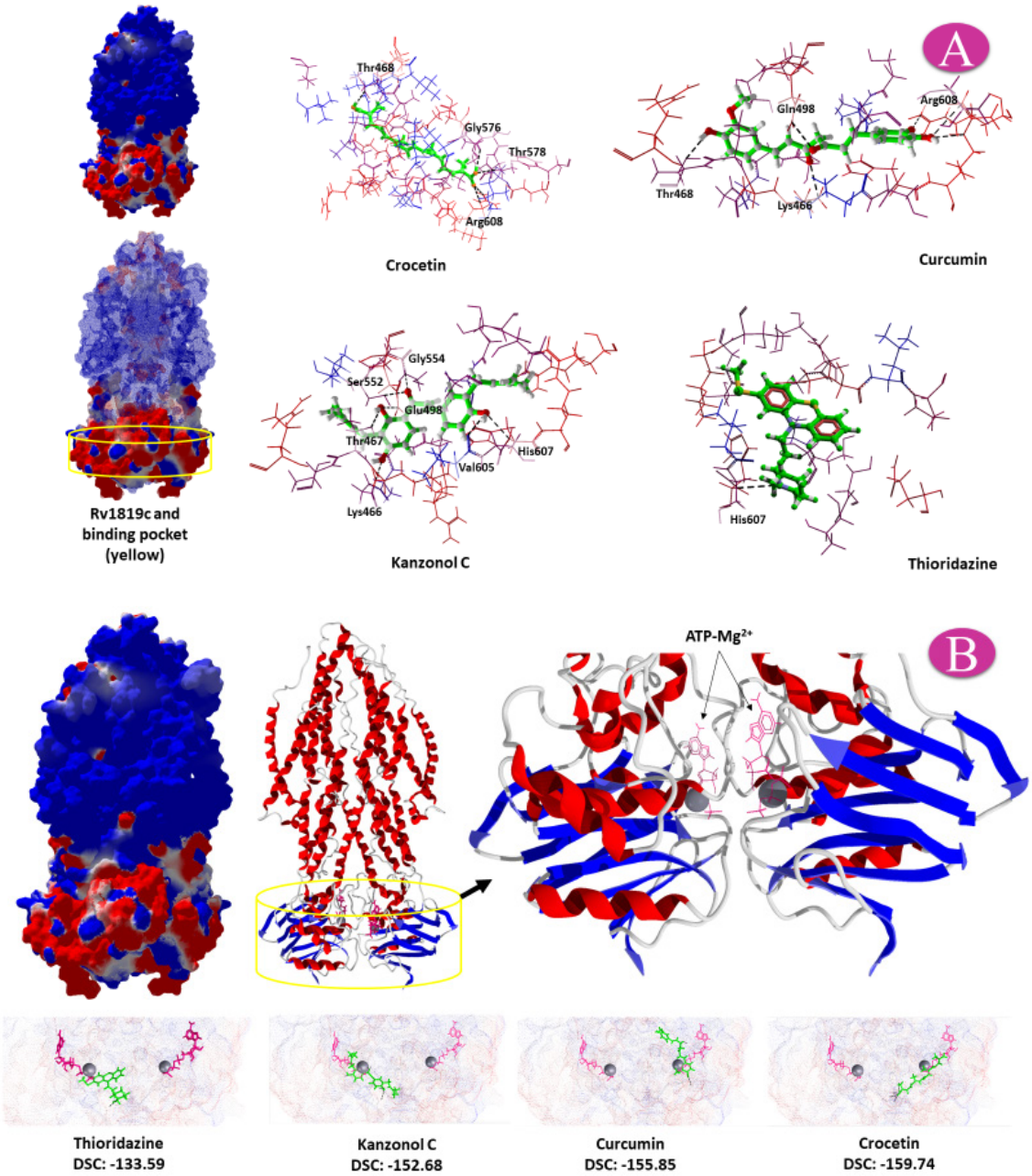

Figure 4) Molecular docking poses and interactions within the ATP-binding site of the Rv1819c protein (PDB: 6TQE). The binding pocket is outlined in yellow. Hydrogen bonds are shown as black dashed lines (thickness indicates strength). The top three compounds, crocetin, curcumin, and kanzonol C, are shown, along with thioridazine, which formed a single hydrogen bond with His607. The native ATP ligand (pink) and the Mg^{2+} ion (gray sphere) are shown within the binding pocket for reference.

protein-ligand interactions are illustrated in Figure 4B.

Molecular dynamics and stability of protein-ligand complexes: The stability of the docked poses was assessed by monitoring the RMSD of the ligand heavy atoms in 200-picosecond molecular dynamics (MD) simulations. A low ligand RMSD value indicates that the ligand position within the binding pocket is stable, validating the initial docking pose [13]. In this study, the observed low and stable ligand RMSD profiles indicated that each complex rapidly reached equilibrium and maintained a consistent binding mode throughout the simulation period. Figure 5 presents the RMSD trajectories of the

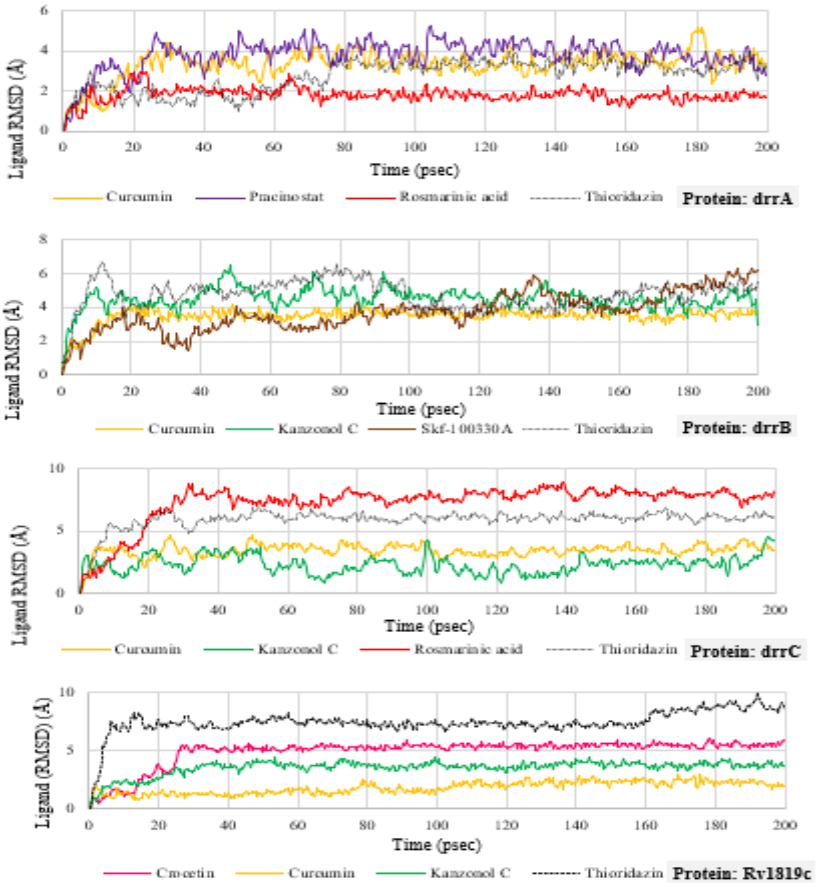

Figure 5) RMSD trajectories from 200 ps molecular dynamics simulations. RMSD values are shown for the top three ligands bound to each protein (DrrA, DrrB, DrrC, Rv1819c), alongside the control compound thioridazine. Low RMSD fluctuations across all simulations indicate stable binding and minimal complex deformation, validating the docking poses.

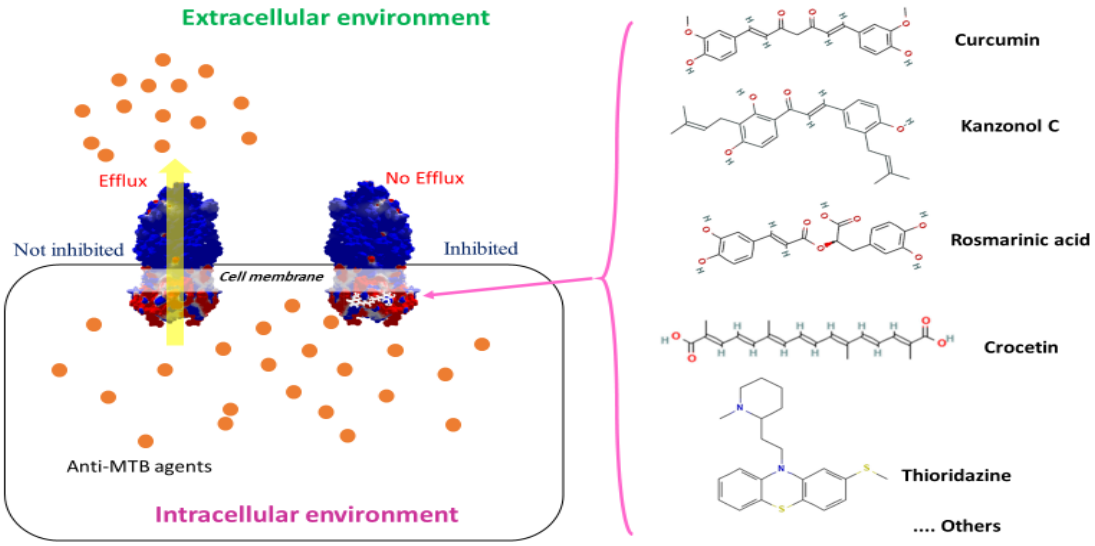

Figure 6) Graphical abstract proposing a mechanism for efflux pump inhibition. Phytochemicals (curcumin, kanzonol C, rosmarinic acid, and crocetin) and known EPIs (e.g., thioridazine) are hypothesized to bind to mycobacterial efflux pumps (e.g., DrrABC, Rv1819c), preventing the extrusion of antibiotics (e.g., isoniazid, rifampin). This inhibition is proposed to increase intracellular antibiotic concentrations, thereby potentiating their efficacy against MTB.

Table 2) Heat-map presentation of cheminformatics analysis, RO5 compliance, and toxicity estimates for the evaluated compounds. Compounds were ranked using a decision score algorithm (see Materials and Methods), with lower scores indicating a more favorable overall profile. The resulting ranking from most to least favorable was as follows: crocetin, curcumin, kanzonol C, rosmarinic acid, pracinostat, thioridazine, and Skf-100330A.

	MW (g/mol)	XLogP3-AA	Hydrogen Bond Donor	Hydrogen Bond Acceptor	Rotatable Bond	TPSA (Å²)	Heavy Atom	Water solubility at 25°C mg/L	Oral rat LD50 (mg/kg)	Bioconcentration factor	Developmental toxicant	Mutagenicity	Toxicity (Cramer rule)	Biodegradability	Cyt P450 metabolism	Protein binding alert	DNA binding alert	Carcinogenicity alert	Known/predicted targets	Decision score
Curcumin	368.4	3.2	2	6	8	93.1	27	35.47	1411.26	13.83	Yes	Neg	High	PRS	PSTQ	Yes	Yes	No	90	89
Rosmarinic acid	360.3	2.4	5	8	7	145	26	1410.37	3481.5	1.11	Yes	Neg	Low	PRS	PSTQ	Yes	Yes	No	109	104
Pracinostat	358.5	3.1	2	4	10	70.4	26	16.34	474.72	7.91	Yes	Pos	High	PRS	PSTQ	Yes	Yes	Yes	114	113
Kanzonol C	392.5	7	3	4	7	77.8	29	0.8	2285.46	17.64	Yes	Neg	High	PRS	PSTQ	Yes	Yes	Yes	99	100
Skf-100330A	333.4	2.4	1	3	6	40.5	25	14.01	557.34	32.77	Yes	Neg	High	PRS	PTQ	Yes	Yes	No	259	252
Thioridazine	370.6	5.9	0	4	4	57.1	25	1.58	1240.64	171.5	Yes	Pos	High	PRS	PSQ	Yes	Yes	No	126	127
Crocetin	328.4	5.4	2	4	8	74.6	24	14.24	6346.98	1.45	Yes	Neg	Low	ESY	PSTQ	No	No	No	85	72
Lower values or Negative																				
Higher values or Positive																				

Abbreviations: Persistent: PRS; Cyt 450: cytochrome P450; PTQS/PTQ/PSQ: primary & secondary & tertiary, and other types of metabolism by Cyt 450

top three compounds bound to DrrA, DrrB, DrrC, and Rv1819c, alongside the control compound (thioridazine).

DrrA complexes: During simulations with the DrrA protein, rosmarinic acid exhibited the highest stability with minimal fluctuations (< 1 Å) in the final picoseconds. Curcumin and pracinostat also demonstrated acceptable stability, maintaining RMSD values below 3 Å at the binding site. Although thioridazine showed low RMSD values, particularly towards the simulation end, the overall results indicated that the modeled DrrA protein was a suitable target for rosmarinic acid, curcumin, and pracinostat.

DrrB complexes: For DrrB, curcumin displayed the lowest RMSD fluctuations, followed by kanzonol C and Skf-100330A. Thioridazine again showed favorable stability with an RMSD value of below 2 Å in the final stages of the simulation.

DrrC complexes: Simulations of DrrC complexes revealed that curcumin and rosmarinic acid had lower RMSD fluctuations than Kanzonol C. Thioridazine exhibited very low RMSD values, which were lower than those of the phytochemicals in this system.

Rv1819c complexes: All three top compounds (crocetin, curcumin, and kanzonol C) bound to the ATP-binding site of the Rv1819c protein (PDB: 6TQE) with low RMSD fluctuations, confirming the stability of these complexes. Thioridazine also demonstrated stable binding with RMSD changes below2 Å. Collectively, these MD simulations support the docking results, indicating good binding stability and favorable interactions between the evaluated phytochemicals and the target efflux pump proteins.

Evaluation of drug-likeness and toxicity: The drug-likeness and toxicity profiles of the lead compounds were quantitatively

assessed using a decision score algorithm detailed in the Methods section, which integrates parameters from Lipinski's rule of five (RO5), ADME properties, and toxicity predictions. Based on this analysis, the compounds were ranked from most to least favorable as follows: crocetin **>** curcumin **>** kanzonol C **>** rosmarinic acid **>** pracinostat **>** thioridazine **>** Skf-100330A (Table 2). Based on this ranking, crocetin was identified as the lead candidate, exhibiting the most promising drug-like properties and the lowest predicted toxicity among the compounds evaluated.

Discussion

The increasing incidence of MDR and extensively drug-resistant (XDR) MTB is a significant global health challenge, underscoring the urgent need for novel therapeutic strategies. A key mechanism of resistance in MTB involves overexpression of EFPs, which reduce intracellular antibiotic concentrations through active extrusion [14]. Among these, ABC transporters utilize primary active transport to efflux a broad spectrum of chemotherapeutic agents, thereby diminishing their clinical efficacy. Beyond antibiotic efflux, these proteins are also crucial for transporting structural lipids across the mycobacterial cell wall. Therefore, inhibiting EFP function may not only restore antibiotic susceptibility but also disrupt essential bacterial processes, including cell division and energy metabolism, potentially shortening the duration of TB therapy [1]. This study focused on ABC transporters DrrA, DrrB, DrrC, and Rv1819c, which are implicated in resistance to anti-TB drugs.

The selection of the drrABC operon was based on STRING database analysis, which confirmed these genes as the most closely associated and co-expressed ABC transporters in MTB H37Rv strain. This computational finding is supported by our previous experimental work, which demonstrated significant overexpression of DrrA and DrrB in MDR-MTB clinical isolates compared to drug-sensitive strains [7]. The DrrABC complex is known to confer a multidrug-resistance phenotype, including resistance to doxorubicin, by translocating substrates across the membrane. Although the evidence for DrrC is less direct, its high co-expression suggests an integral role in this complex. Therefore, it was hypothesized that targeting these specific EFPs could effectively counteract efflux-mediated resistance.

Molecular docking and dynamics simulations revealed that several phytochemicals, including curcumin, rosmarinic acid, and crocetin, bound with high affinity to DrrA, DrrB, DrrC, and Rv1819c and formed stable complexes. Notably, many of these compounds exhibited improved binding characteristics compared to the control efflux pump inhibitor (thioridazine). Furthermore, ADMET and drug-likeness profiling showed that these phytochemicals, particularly crocetin, possessed promising toxicity profiles and pharmacological properties. These findings suggest that the identified phytochemicals are promising candidates for adjuvant therapy aimed at inhibiting MTB efflux pumps. By potentiating the activity of conventional antibiotics, such compounds could provide a strategic pathway for overcoming multidrug resistance in tuberculosis. In summary, the integrated computational analysis used in this study identified several phytochemicals as promising candidates for inhibiting key efflux pumps in *M. tuberculosis*. Co-expression data retrieved from the STRING database identified DrrC, alongside DrrA and DrrB, as a critical component of the ABC transporter system and a potential target for anti-efflux therapeutics.

Molecular docking studies revealed that curcumin, kanzonol C, rosmarinic acid, and

crocetin exhibited the highest binding affinities to the modeled structures of DrrA, DrrB, DrrC, and the known Rv1819c protein. Notably, all of these natural compounds demonstrated higher docking scores compared to the control efflux pump inhibitor, thioridazine. The stability of these ligand-protein complexes was further validated by molecular dynamics simulations, which showed low RMSD fluctuations at the binding sites. Furthermore, a comprehensive evaluation of toxicity and drug-likeness profiles indicated that crocetin, curcumin, and kanzonol C presented the most favorable profiles among the compounds tested. A proposed mechanism, illustrated in Figure 6, suggests that these phytochemical inhibitors could potentiate conventional anti-TB therapies by blocking efflux-mediated antibiotic extrusion, thereby increasing their intracellular concentration and efficacy. The findings are supported by existing literature on the antimycobacterial properties of these compounds.

The efficacy of curcumin and its derivatives has been previously documented by mechanisms including synergistic effects with antibiotics, inhibition of biofilm formation, and modulation of host immune responses [15], supporting its potential as an adjuvant therapy, as demonstrated in a murine TB model [16]. Similarly, Kanzonol C has been reported to inhibit MTB-H37Rv reverse transcriptase [17].

Rosmarinic acid and its methyl ester derivative exhibit direct inhibitory effects against both drug-sensitive and MDR-MTB strains, with proposed targets including lipoamide dehydrogenase, a component crucial for defense against host reactive nitrogen intermediates stress [18, 19], and the stress protein Rv2623, which is implicated in persistence and chronic infection [18, 20, 21].

The potential of crocetin as an anti-mycobacterial agent is further supported by prior research. A docking study by Pradhan and colleagues (2023) demonstrated that crocetin bound to protein kinase G in MTB, a virulence factor that enables bacterial persistence by inhibiting lysosomal degradation [22]. Furthermore, Hussain et al. (2014) reported that hexane and methanol extracts of *Crocus sativus* (saffron), from which crocetin is derived, inhibited the growth of MTB H37Rv on Löwenstein-Jensen medium by 66-78% [23]. Our computational results align with these findings, suggesting that the selected phytochemicals, including crocetin, may enhance drug retention within the mycobacterial cell by inhibiting efflux pumps, thereby potentially resensitizing MDR strains to conventional antibiotics.

Collectively, the evidence implies that curcumin, kanzonol C, rosmarinic acid, and crocetin exert multi-faceted effects on MTB growth and pathogenesis. While their direct anti-MTB properties have been documented [15-18, 22, 23], the present study specifically demonstrated their promising potential as EPIs. This action could yield significant synergistic effects when co-administered with first-line anti-TB antibiotics such as isoniazid and rifampin. Notably, efflux inhibition by curcumin and rosmarinic acid has been previously reported in other bacterial systems [24, 25], bolstering the plausibility of our findings. The widespread use of these compounds in food and cosmetic products is in contrast to the contradictory pharmacological effects observed due to their dietary intake. This discrepancy is multifactorial and primarily stems from the challenge of achieving a pharmacologically relevant concentration at the site of infection through diet alone. Key determinants of efficacy, including bioavailability, metabolic stability, route of administration, and tissue penetration, could not be optimized through casual consumption, explaining the lack of consistent anti-infective outcomes.

The novelty of this study lies in the inte-

grated application of bioinformatics and cheminformatics methodologies. Co-expression analysis, homology modeling, molecular docking, molecular dynamics simulations, and ADMET profiling were combined to systematically evaluate phytochemicals against the target proteins. This comprehensive multi-stage screening strategy identified curcumin, kanzonol C, and crocetin as the most promising drug candidates.

This framework allowed us to prioritize compounds not only based on binding affinity but also based on their stability and drug-like properties, de-risking the selection process for future experimental work. Therefore, this study provides a robust computational foundation for subsequent *in vitro* and *in vivo* studies to evaluate the therapeutic potential of these promising candidates, particularly curcumin, kanzonol C, rosmarinic acid, and crocetin, as components of a novel combination therapy against MDR-TB.

Although this *in silico* study provides a strong rationale for phytochemical-based EPIs, several limitations must be acknowledged. Our computational predictions require experimental validation to account for complex *in vivo* factors not captured by the models, such as metabolic stability of the compounds, expression levels of efflux pumps within granulomas or host environments, bioavailability, and achievable concentrations at the site of infection. Although validated, our homology models are approximate; high-resolution crystal structures provide a more definitive basis for docking studies.

Future work must prioritize *in vitro* and *ex vivo* assays to confirm efflux inhibition and synergism with standard antibiotics. The use of techniques such as site-directed mutagenesis of identified binding residues and surface plasmon resonance to measure binding affinity are essential next steps. Ultimately, efficacy and toxicity must be evaluated in appropriate animal models before any clinical investigation of these compounds as adjuvant therapies for MDR/XDR -TB.

Conclusion

Our integrated *in silico* analysis identified curcumin and kanzonol C as the top-performing phytochemicals, demonstrating the highest binding affinity and stability to the modeled structures of the DrrA, DrrB, and DrrC efflux pumps. Given the crucial role of these proteins in MTB antibiotic resistance, administration of curcumin, kanzonol C, or a combination of them could potentially enhance therapeutic outcomes by inhibiting efflux activity. Therefore, these phytochemicals are proposed as strong candidates for adjuvant therapy to potentiate the efficacy of first-line anti-TB antibiotics, such as isoniazid and rifampin. Furthermore, this study highlighted crocetin as a highly promising inhibitor of the well-characterized Rv1819c ABC transporter, a protein known to extrude a broad spectrum of compounds, including aminoglycosides and fluoroquinolones. Crocetin yielded the most favorable DSC for this target.

Based on these findings, future *in vitro* and *ex vivo* studies are recommended to evaluate the potential of these phytochemicals, both individually and in complex formulations, to resensitize drug-resistant MTB to conventional antibiotics.

Acknowledgments

The authors utilized DeepSeek AI (https://chat.deepseek.com/) solely for the purpose of language editing and grammatical correction of the manuscript text. The AI was prompted to “check and rewrite sentences considering English language grammar and scientific writing for publication in a scientific journal”. The conceptualization, study design, analysis, interpretation of data, and scientific content are solely the work of the authors. No artificial intelligence tool was

used in any part of the research itself.

Ethical statement: None declared by authors.

Authors' contributions: SA.M contributed to proofreading the article, A.Acontributed to the study design, bioinformatics analysis, and manuscript preparation. Z.A and F.P contributed to bioinformatics analysis and manuscript preparation.

Competing interests: The authors declare that they have no competing interests.

Funding: None declared by Authors.

Availability of data and materials: All data generated or analyzed during this study are included in this published article. Any additional raw data supporting the findings are available from the corresponding author email upon reasonable request.

Consent to participate: No participants and not applicable.

Abbreviations

6-Dpg: 6-(3,3-Diphenylpropyl) guvacine; Å: Angstrom; ABC: doxorubicin resistance ATP-binding cassette; ADME: adsorption, distribution, metabolism, excretion; ANOVA: analysis of variance; ATP: adenosine triphosphate; drrA/B/C: doxorubicin resistance ATP-binding gene A/B/C; DrrA/B/C: doxorubicin resistance ATP-binding protein A/B/C; Cyt-P450: cytochrome P450; CID: compound identification; DSC/DSCs: docking score/s; EFP: efflux pump; EPIs: EFP inhibitors; GMQE: global model quality estimation; GUI: graphic user interface; MD: molecular dynamics; MTB: *Mycobacterium tuberculosis*; RO5: Lipinski's rule of 5; PDB: protein data bank; SID: sequence identity; TB: tuberculosis; MDR-TB: multidrug-resistant *Mycobacterium tuberculosis*; MW: molecular weight; RMSD: root means square deviation; T.E.S.T: Toxicity Estimation Software Tool; TPSA: total polar surface area, WHO: World Health Organization; XDR: extensively drug-resistant

References

1. Remm S, Earp JC, Dick T, Dartois V, Seeger MA. Critical discussion on drug efflux in Mycobacterium tuberculosis. FEMS Microbiol Rev. 2022;46(1):fuab050.
2. World Health Organization. Global tuberculosis report 2024. Geneva: World Health Organization; 2024.
3. Laborda P, Molin S, Johansen HK, Martínez JL, Hernando-Amado S. Role of bacterial multidrug efflux pumps during infection. World J Microbiol Biotechnol. 2024;40(7):1-10.
4. Duda-Madej A, Viscardi S, Niezgódka P, Szewczyk W, Wińska K. The impact of plant-derived polyphenols on combating efflux-mediated antibiotic resistance. Int J Mol Sci. 2025;26(9):4030.
5. Sowajassatakul A, Prammananan T, Chaiprasert A, Phunpruch S. Overexpression of eis without a mutation in promoter region of amikacin-and kanamycin-resistant Mycobacterium tuberculosis clinical strain. Ann Clin Microbiol Antimicrob. 2018;17(1):1-7.
6. Choudhuri BS, Bhakta S, Barik R, Basu J, Kundu M, Chakrabarti P. Overexpression and functional characterization of an ABC (ATP-binding cassette) transporter encoded by the genes drrA and drrB of Mycobacterium tuberculosis. Biochem J. 2002;367(1):279-85.
7. Khosravi AD, Sirous M, Absalan Z, Tabandeh MR, Savari M. Comparison of drrA and drrB efflux pump genes expression in drug-susceptible and -resistant Mycobacterium tuberculosis strains isolated from tuberculosis patients in Iran. Infect Drug Resist. 2019;12:3437-44.
8. Zheng M, Lupoli T. Counteracting antibiotic resistance enzymes and efflux pumps. Curr Opin Microbiol. 2023;75:102334.
9. Compagne N, da Cruz AV, Müller R, Hartkoorn RC, Flipo M, Pos KM. Update on the discovery of efflux pump inhibitors against critical priority gram-negative bacteria. Antibiotics. 2023;12(1):180.
10. Schwede T, Kopp J, Guex N, Peitsch MC. SWISS-MODEL: An automated protein homology-modeling server. Nucleic Acids Res. 2003;31(13):3381-5.
11. Grimsey EM, Piddock LJ. Do phenothiazines possess antimicrobial and efflux inhibitory properties? FEMS Microbiol Rev. 2019;43(6):577-90.
12. Rempel S, Gati C, Nijland M, Thangaratnarajah C, Karyolaimos A, de Gier JW, et al. A mycobacterial ABC transporter mediates the uptake of hydrophilic compounds. Nature. 2020;580(7803):409-12.
13. Arnittali M, Rissanou AN, Harmandaris V. Structure of biomolecules through molecular

dynamics simulations. Procedia Comput Sci. 2019;156:69-78.
14. Devita N. World TB Day 2025: Advancing the fight against tuberculosis through science and nature. JKKI. 2025;16(1):1-4.
15. Barua N, Buragohain AK. Therapeutic potential of curcumin as an antimycobacterial agent. Biomolecules. 2021;11(9):1278.
16. Lara-Espinosa JV, Arce-Aceves MF, López-Torres MO, Lozano-Ordaz V, Mata-Espinosa D, Barrios-Payán J, et al. Effect of curcumin in experimental pulmonary tuberculosis: Antimycobacterial activity in the lungs and anti-inflammatory effect in the brain. Int J Mol Sci. 2022;23(4):1964.
17. Wang D, Liang J, Zhang J, Wang Y, Chai X. Natural chalcones in Chinese materia medica: Licorice. Evid Based Complement Alternat Med. 2020;2020(1):3821248.
18. Sarkar N, Khanal P, Rawat R, Dey YN, Roy KK. Rosmarinic acid and its derivative's duel as antitubercular agents: Insights from computational prediction to functional response in vitro. J Biomol Struct Dyn. 2023:42(23):12720-9.
19. Venugopal A, Bryk R, Shi S, Rhee K, Rath P, Schnappinger D, et al. Virulence of Mycobacterium tuberculosis depends on lipoamide dehydrogenase, a member of three multienzyme complexes. Cell Host Microbe. 2011;9(1):21-31.
20. Drumm JE, Mi K, Bilder P, Sun M, Lim J, Bielefeldt-Ohmann H, et al. Mycobacterium tuberculosis universal stress protein Rv2623 regulates bacillary growth by ATP-Binding: Requirement for establishing chronic persistent infection. PLoS Pathog. 2009;5(5):e1000460.
21. Glass LN, Swapna G, Chavadi SS, Tufariello JM, Mi K, Drumm JE, et al. Mycobacterium tuberculosis universal stress protein Rv2623 interacts with the putative ATP binding cassette (ABC) transporter Rv1747 to regulate mycobacterial growth. PLoS Pathog. 2017;13(7):e1006515.
22. Pradhan S, Nautiyal V, Dubey R. Molecular docking of some active ingredients of oblation materials used in Yajña against tuberculosis causing Mycobacterium tuberculosis. Vegetos. 2023;36(4):1557-65.
23. Hussain S, Haq A, Nisar M, Ahmad T, Bhardwaj P. Evaluation of in-vitro anti-mycobacterial activity and isolation of active constituents from Crocus sativus L.(Iridaceae). Asian J Med Pharm Res. 2014;4(2):130-5.
24. Negi N, Prakash P, Gupta ML, Mohapatra TM. Possible role of curcumin as an efflux pump inhibitor in multidrug resistant clinical isolates of Pseudomonas aeruginosa. J Clin Diagn Res. 2014;8(10):DC04.
25. Ekambaram SP, Paramasivam S, Perumal SS, Dhakshinamurthy SS. Rosmarinus officinalis L.: A source of potential antimicrobial agents for combating antimicrobial resistance. Lett Appl NanoBioScience. 2024;13(1):1-25